



Evaluation the efficiency of a parametric model based on MODIS data for solar radiation estimation in comparison with some empirical models

Bijan Sedaqat Masabi¹ · Zahra Aghashariatmadari² · Somayeh Hejabi³

Received: 26 October 2020 / Accepted: 30 June 2021 / Published online: 27 July 2021
© Saudi Society for Geosciences 2021

Abstract

In the present study, the output of several empirical models for estimating solar radiation and the output of a model based on data obtained from moderate resolution imaging spectroradiometer (MODIS) sensor (parametric model) are compared with ground observational station to introduce a suitable algorithm for estimating solar radiation in the studied stations. For this purpose, first the selected empirical models were calibrated according to the climatic conditions of the study area and then used to estimate solar radiation. To this aim, empirical models were evaluated based on suitably partitioned datasets. 75% of the total data were utilized for training phase and the remaining 25% data were used for testing phase and conducting statistical analysis. In the next step, the parametric model (SBDART) were tested and used for predicting the solar radiation data in target stations. The results indicated that the R^2 value of models vary between 0.25 to 0.95, most of which are related to the Santa Barbara DISORT (discrete ordinates radiative transfer) atmospheric radiative transfer (SBDART) ($R^2=0.95$) and calibrated Angstrom models ($R^2=0.89$), respectively. The mean absolute percentage error of the SBDART model is significantly different from other models (MAPE=4.3%). After that, the lowest MAPE (mean absolute percentage error) is related to the Angstrom model (MAPE =5.98%). In addition, the parametric model is more efficient on cloudy days than on cloudless days so that the calculated RMSE (root mean square error) and MBE (mean bias error) indices are 9.07 W/m².day and -0.72 W/m².day for cloudy days, and 19.77 W/m².day and 3.60 W/m².day for cloudless days. In contrast, the empirical Angstrom-Prescott model had better results with observational data on cloudless days so that the indices were RMSE =43.60 W/m².day and MBE =34.25 W/m².day for cloudy days, and RMSE =29.56 W/m².day and MBE= 6.19 MJ/m².day for cloudless days.

Keywords Solar radiation estimation, · MODIS sensor, · Parametric model (SBDART), · Empirical models

Introduction

Solar energy is considered as one of the most reliable sources of renewable energy in the world. The development of this

Responsible Editor: Zhihua Zhang

✉ Zahra Aghashariatmadari
zagha@ut.ac.ir

- ¹ MSc student of Agrometeorology, Irrigation and Reclamation Engineering Department, University College of Agriculture and Natural Resources, University of Tehran, Karaj, Iran
- ² Irrigation and Reclamation Engineering Department, University College of Agriculture and Natural Resources, University of Tehran, Karaj, Iran
- ³ Department of Water Engineering, Faculty of Agriculture, Urmia University, Urmia, Iran

source of energy facilities in a place is possible with the assessments made of the solar energy potential of that place. So, modeling and predicting the amount of energy emitted from the sun and high accuracy in evaluating this resource, has provided an important area of research and accelerates technology advancement by having a positive impact on decision-making and reducing uncertainty in development planning (Deo and Sahin 2017). Unfortunately, due to financial, technical or organizational constraints, there are no solar radiation stations in most parts of the world and some existing radiometers are not accurate enough and their data are erroneous. Therefore, in addition to the methods based on the measured values of radiation, several other methods including the use of artificial intelligence (Deo and Sahin 2017; Ghimire et al. 2019; Mohammadi and Aghashariatmadari 2020), satellite images (Qin et al. 2011; Kim and Liang 2010), physical and statistical modeling based on the measured values of

meteorological factors (El-Metwally 2004; Liu et al. 2010; Demirhan et al. 2013; Sun et al. 2015), neural networks (Alsina et al. 2016; Renno et al. 2015) and radiation transfer models (Chen et al. 2016; Benajes et al. 2015; Chen et al. 2015) were proposed. Also, several large-scale models are used to fill the data measurement gap, extend data measurement periods, and estimate radiation at other meteorological stations where radiation is not measured. Although the data sets provided by this method contain a large amount of measured radiation data, their main part consists of modeled values (Muneer 2004). Additionally, over the years, remote sensing, satellites, and their data have revolutionized the field of meteorological and climatological studies. The ability to collect continuous temporal and spatial signals above the atmosphere is considered as one of the advantages of remote sensing that makes it possible to estimate radiation in remote areas where radiation stations are scattered. Another strength of satellite methods is their ability to accurately plot relative differences between adjacent areas, although absolute accuracy may not be perfect for each point. However, this method was proven to be a reliable reference for describing the micro-climatic properties of radiant energy.

Despite the importance of solar radiation on ground processes, little effort has been made to develop and produce high-resolution geographical maps around the world. Due to the limitations of terrestrial database models, a number of models were developed to estimate radiation on the planet's horizontal surfaces using solar or terrestrial satellites at different resolutions (Journée and Bertrand 2010). Many models of radiation estimation based on satellite imagery can produce daily radiation with relatively high accuracy compared to Pyranometric data. There are generally three different ways to estimate solar radiation from satellite data: A) Statistical modeling such as the HELIOSAT model for METEOSAT satellites (Rigollier et al. 2004) and the cloud-cover index model (Perez et al. 2002); B) physical modeling using a complex radiation transfer model (Kim and Liang 2010); and C) parameterized radiation transmission model (Yang et al. 2006). So far, the models designed to estimate radiation from satellite observations are in a diverse range from purely physical models to absolute empirical models including the practical model proposed by Perez et al. (2002) and Janjai et al. (2005). Pure physical models attempt to describe radiation reaching the Earth's surface by the radiation transfer equation, which requires complete knowledge of tuning and calibration of satellite images and accurate information of the constituents of the atmosphere (Raschke and Preuss 1979; Gautier et al. 1980; Schillings et al. 2004a, b). Empirical/statistical models, on the other hand, can involve establishing a simple regression relationship between satellite observational values and terrestrial measurements (Tarpley 1979; Cano et al. 1986). Further, hybrid models use the approach of simple physical models with some fitting to the observations. Perez et al. (1997) and

Zelenka et al. (1999) indicated that solar radiation data estimated by satellite imagery are more accurate than data interpolated through modern radiometric network measurements. In addition, Perez et al. (2002) reported that hourly satellite estimates are more accurate than empirical methods based on ground station measurements at a distance of 25 km from each other compared to field measurements. Lotfi (2012) estimated the net radiation values of Fars province using MODIS sensor images and showed that the. Based on the results, the estimated values show a $\pm 13\%$ error and concluded that this error rate is acceptable given the area of satellite cells (6.5 ha). Zhang et al. (2014) calculated the total amount of solar radiation for the Tibetan Plateau using MODIS sensor data and hybrid parametric model to provide the results with more spatial resolution for short-wavelength radiation than its predecessors. Ryu et al. (2018) combined an atmospheric radiative transfer model with an artificial neural network (ANN) to estimate shortwave solar radiation. A series of MODIS products were used as inputs to run the ANN. Results showed that the developed products will be useful in solar energy investigations. Ghimire et al. (2019) designed algorithms based on deep belief and neural networks and trained them with MODIS satellite data in Australia to predict the monthly ground solar radiation. Results showed that the proposed method can be adopted to estimate solar radiation in regions where it is impossible to setting up monitoring data acquisition instruments. Bamehr and Sabetghadam (2021) developed models using multiple linear regression method and artificial neural networks using some atmospheric properties extracted from MODIS and ozone monitoring instrument (OMI) in Mashhad. Results indicated that the estimates were more accurate using the artificial neural networks than the regression method and in both methods, the accuracy of estimation improves when cloud fraction is used as a predictor. Other studies in this area were conducted by López and Batlles (2014), Qin et al. (2011) and Gao et al. (2015).

Iran is among the countries with high received of solar radiation, which makes it possible to provide a significant part of its energy demands through this clean energy source (Aghashariatmadari 2011). However, the country's radiation network is weak and the number of radiation stations, despite the great importance of this variable, is very small and the stations are scattered throughout the country. The use of experimental models to estimate radiation is common, but these models, despite their sometimes high errors, need to achieve some meteorological variables in the study period. By increasing the access to satellite data, an opportunity becomes available which should be used to the fullest, especially for an important variable such as solar radiation, which is an input for a large number of climatic and global models. The ability to collect continuous temporal and spatial signals above the atmosphere is considered as one of the advantages of remote sensing and satellite images. Moreover, the minimum data

requirement is considered as another key advantages of this method, especially in data-scarce regions. This feature makes it possible to estimate radiation in remote areas where radiation stations are scattered. Accordingly, the importance of the present study is to evaluate and compare the efficiency of solar radiation empirical models on the ground with a selected satellite based model named SBDART presented by Ricchiazzi et al. 1998. In this regard, the data measured in four selected radiometric stations are compared with the radiation values obtained from the implementation of algorithms based on satellite images and a suitable algorithm for estimating radiation in the studied stations is introduced based on the analysis of statistical measures.

Materials and method

Study area and statistical specifications of the data

In this study, the synoptic stations in Zanjan, Kerman, Mashhad, and Yazd were selected as study stations, and the studies were performed from statistical quality control to the extraction of relationships using daily data from these stations during 2007–2015.

Daily weather data of four synoptic stations of Kerman (latitude 30.25°N, longitude 56.97°E, altitude 1753.8 meter above sea level), Mashhad (latitude 36.27°N, longitude 59.63°E, altitude 999.2 m asl), Zanjan (latitude 36.68°N, longitude 48.48°E, altitude 1663.0 m asl) and Yazd (latitude 31.90°N, longitude 54.28°E, altitude 1237.2 m asl) have been received in the 8-year period of 2015–2007 through the Iranian Meteorological Organization (IRIMO) (Fig. 1 and Table 1). The climate of stations varies from arid to semi-arid. Zanjan station represent the semi-arid climate type based on De Martonne's classification. The annual precipitation of the city is about 303.5 mm and the minimum and maximum mean annual temperatures are about 4.3°C and 18.4 °C, respectively. Kerman station represent the arid climate type. The annual

precipitation of the city is about 142.5 mm and the minimum and maximum mean annual temperatures are about 7.1°C and 24.9°C, respectively. Mashhad is another station that its daily mean annual temperature amplitude is about 13.8°C. The total sum of its precipitation is 246.9 mm and located in semi-arid climate. The final station is Yazd. Its climate is defined by dry. The annual precipitation of the city is about 55.3 mm on average, and the maximum and minimum annual temperatures are about 26.8°C and 12.2°C, respectively. The predominant common crop of the studied cities, in addition to their specific crops, is wheat.

The long-term statistical period of the radiation data is considered as a basis for selecting these stations. At this point, first, the long-term statistics of the meteorological stations on a daily basis were received from the meteorological organization and a yearly-classified database was formed. This bank includes data on total solar radiation (R_s), radiation received on the horizontal surface above the atmosphere (R_0), sunshine hour fraction, horizontal visibility and cloudiness. Data quality control was performed based on Moradi et al. (2009) quality control algorithm. Only the variables related to radiation (total radiation and number of hours of sunshine) of all meteorological data received had statistical deficiencies. Therefore, regarding the purpose of the study, the quality control of radiation statistics was performed with high accuracy.

Empirical models

Angstrom relationship (1924)

Angstrom Relationship is a simple linear relation which expresses the amount of sunlight on a horizontal surface by its ratio to the amount of radiation on a clear, cloudless day with a clear sky. This relationship is the basis of many radiation estimation models. In his proposed relation, Angstrom introduces the radiation fraction ($\frac{R_s}{R_c}$) as a linear function of the

Table 1 Statistical specifications of the data used in the studied stations

| Station | Latitude | Altitude | Elevation (m) | Major Cultivation | Minimum Temperature (°c) | Maximum Temperature (°c) | Precipitation (mm) | Relative Humidity (%) | Sunshine hour (hr) | Climate type (Demartone) |
|---------|----------|----------|---------------|--------------------------------|--------------------------|--------------------------|--------------------|-----------------------|--------------------|--------------------------|
| Zanjan | 36.68 | 48.48 | 1663.0 | Wheat, apple, grape, Olive | 4.3 | 18.4 | 303.5 | 56 | 1810.9 | Semi-arid |
| Kerman | 30.25 | 56.97 | 1753.8 | Wheat, Dates, pistachios | 7.1 | 24.9 | 142.5 | 26 | 2398.4 | Arid |
| Mashhad | 36.27 | 59.63 | 999.2 | Wheat, barley, canola, saffron | 7.6 | 21.4 | 246.9 | 48 | 2497.8 | Semi-arid |
| Yazd | 31.90 | 54.28 | 1237.2 | Pomegranate, wheat, pistachio | 12.2 | 26.8 | 55.3 | 27.5 | 2040.7 | Arid |

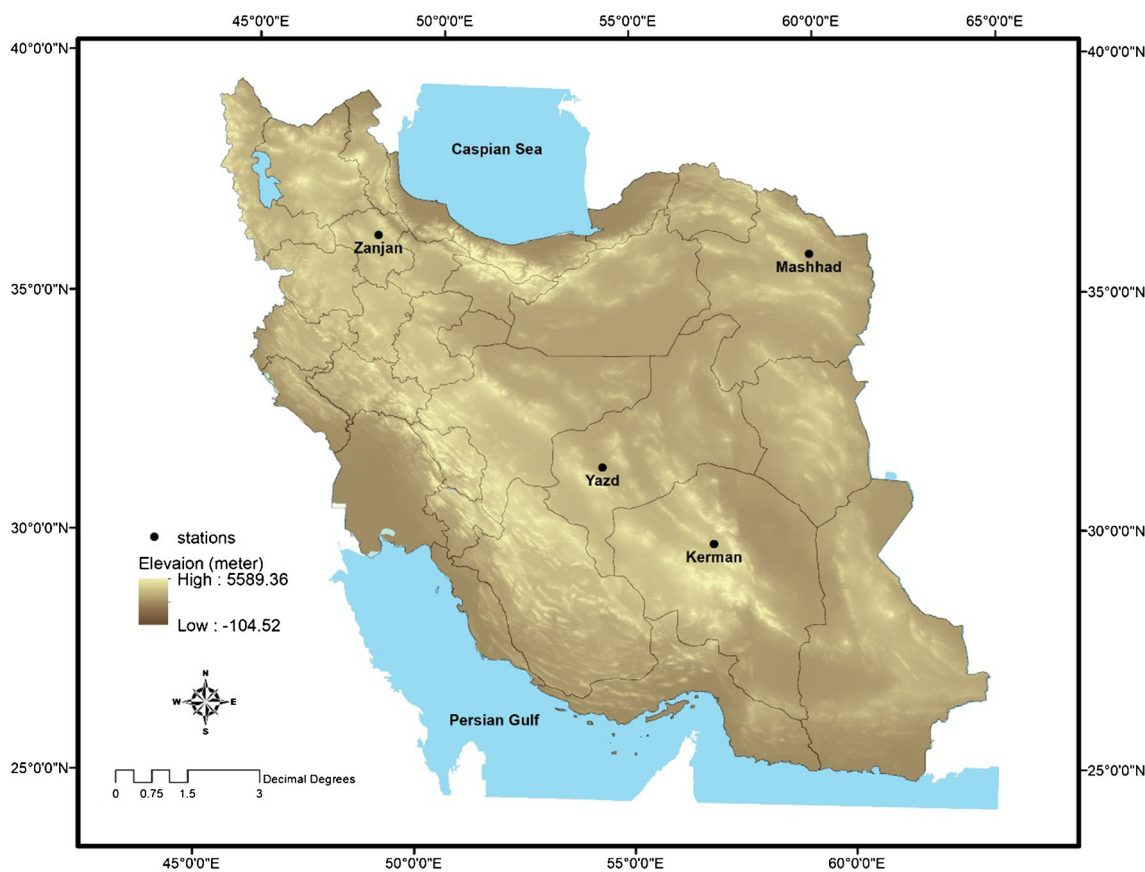


Fig. 1 Solar radiation stations' distribution

fraction of sunshine hours ($\frac{n}{N}$).

$$\frac{R_s}{R_c} = f\left(\frac{n}{N}\right) = a + b \frac{n}{N} \tag{1}$$

where R_c is the total radiation on a clear, cloudless day with a clear sky; R_s is the total radiation received from the sun on a horizontal surface on the earth's surface; n is the actual number of hours of solar radiation, N is the number of theoretical hours of solar radiation calculated from astronomical relationships, and, a, b are the empirical coefficients which should be calculated with the help of the statistical period of measured radiation data and solar hours. The coefficients used in the Angstrom formula vary depending on atmospheric conditions (humidity, dust, etc.) and solar radiation (latitude and month of the year).

These relationships are used when the amount of R_c (radiation received on the horizontal surface of the earth in perfectly clear and transparent sky conditions) is known, which is difficult to determine. In order to overcome this limitation, several researchers suggested the use of received radiation on the horizontal surface above the atmosphere (R_0) instead of (R_c).

$$\frac{R_s}{R_0} = \left(0.22 + 0.54 \frac{n}{N}\right) \tag{2}$$

Accordingly, the equation introduced by Angstrom was first modified in 1940 by Prescott. In his proposed equation, Prescott (1940) substituted the radiation received from the sun above the atmosphere on the horizontal surfaces for the radiation in clear and transparent sky conditions, and the coefficients a, b were 0.22 and 0.54, respectively, by using the data of Mont weather station (USA). The Angstrom equation was widely used after the Prescott correction as the Angstrom-Prescott equation.

In the cases which radiation data are not available and calibration is not performed to correct the parameters, the values $a = 0.25, b = 0.5$ are used (Allen et al. 1998). Considering the importance of pure solar radiation in the equation used to estimate evapotranspiration and water requirement of plants and other applications of solar radiation, it is necessary to calibrate and define the values of coefficients in each area according to the conditions of that area.

Swartman and Ogunlade model

Swartman and Ogunlade (1967) investigated the effect of relative humidity on the received radiation and introduced some equation in this respect. They showed that these equations give better estimates of solar radiation intensity than the

single-parameter relationship in tropical countries.

$$R_s = 18.765 \left(\frac{n}{N}\right)^{0.36} (RH)^{-0.15} \tag{3}$$

$$R_s = 14.451 + 174.593 \left(\frac{n}{N}\right) - 10.137(RH) \tag{4}$$

where *RH* is the relative humidity.

Hargreaves and Samani model

Hargreaves and Samani (1982) presented a simple empirical model to simulate daily solar radiation to estimate evapotranspiration when only minimum and maximum temperatures are available. They hypothesized that the transience of atmosphere on a given day was proportional to the second root of the difference between the minimum and maximum daily temperatures (Celsius):

$$R_s = K_r (T_{max} - T_{min})^{0.5} R_n \tag{5}$$

where *R_n* is the total radiation received from the sun on a horizontal surface above the earth atmosphere, *R_s* indicates the total radiation received from the sun on a horizontal surface on the earth surface, and *K_r* is considered as an experimental constant to consider the effect of dust in the atmosphere and the change in water vapor pressure with altitude.

Gopinathan model

Gopinathan (1988) proposed the equations to estimate the regression coefficients *a* and *b* of angstrom type correlations for predicting monthly mean daily global solar radiation. These equations developed using average monthly values of altitude (m), $\frac{n}{N}$ and $\frac{R_s}{R_0}$ variables with the aim to be applicable to all parts of the world to compute global solar radiation.

$$\frac{R_s}{R_n} = a + b \left(\frac{n}{N}\right) \tag{6}$$

$$a = 0.265 + 0.070h - 0.135 \left(\frac{n}{N}\right) \tag{7}$$

$$b = 0.401 + 0.108h - 0.325 \left(\frac{n}{N}\right) \tag{8}$$

El-Metwally model

El-Metwally (2004) proposed the 4 Parameter Polynomial model in Egypt. The methods use ground-based measurements of maximum and minimum temperature, daily mean of cloud cover and extraterrestrial global radiation.

$$R_s = aR_o + bT_{max} + cT_{min} + d_{cm} + e \tag{9}$$

Where *a, b, c, d, e* are the experimental constants, *T_{max}* and *T_{min}* the air temperature maximum and minimum (°c) and *cm* is average cloud cover (Okta).

Garg model

Water vapor affects the permeability of the atmosphere. Calculations by Tamm and Thormalla (1992) indicated that increasing water vapor from 1 to 4 cm of water in a vertical bar reduces the average daily total radiation in a cloudless sky by 5.6%. Accordingly, Garg and Garg (1982) introduced their model by involving water vapor content in the structure of the relationship:

$$\frac{R_s}{R_0} = \left(E + F \left(\frac{n}{N}\right) + H \cdot w_{at} \right) \tag{10}$$

In this regard, *R_s* the average monthly total solar radiation (*Mjm⁻²day⁻¹*), *w_{at}* is the content of atmospheric water vapor per unit volume of air (*g^m-³*) and *E, F, H* are the coefficients of the relationship. *w_{at}* is calculated based on the equation suggested by Hussain (1984):

$$w_{at} = RH(4.7923 + 0.3647T_a + 0.0055T_a^2 + 0.0003T_a^3) \tag{11}$$

where *RH* indicates relative humidity (%) and *T_a* is average air temperature (degrees Celsius).

Finally, the coefficients of selected empirical models of radiation estimation were calibrated based on meteorological and geographical conditions in Iran (Table 2).

MODIS sensor data

Data regarding measured radiation on the ground was used as well as MODIS sensor data. MODIS sensors are installed on Aqua and Terra satellites. The images used by the MODIS sensor of Aqua and Terra satellites in the form of MODIS products were received in the 8-year period of 2015–2007 through the websites <http://modis.gsfc.nasa.gov> and <https://reverb.echo.nasa.gov>. Due to the two sun-synchronous satellites, the Terra satellite images were taken at 10:30 a.m. and the Aqua satellite images at 13:30 local time on a daily basis. The studied days were selected from the days approved in the quality control tests in such a way that at least one day as its representative was checked for each month between mid-March and mid-August for a period of eight years. Satellite data were extracted from level-2 MODIS sensor products stored in HDF files, from which atmospheric and terrestrial specifications can be obtained. The total possible amount of precipitable water from the atmosphere was extracted from the data (MOD/MYD05) and the visual thickness of the cloud was derived from the products (MOD/MYD06). Similarly, MOD/MYD04 data were used due to lack of observation of variables such as aerosol values. In the case of high

Table 2 Calibrated models in Iran Radiation Measurement Network

| Model Name | Relationship |
|-----------------------|--|
| Angstrom (FAO) | $R_s R_0 = 0.25 + 0.5 \frac{n}{N}$ |
| Angstrom (calibrated) | $R_s R_0 = 0.274 + 0.458 \frac{n}{N}$ |
| Swartman | $R_s = 288 + 433 \frac{n}{N} - 2.96RH$ |
| Gopinathan | $R_s R_0 = [0.194 + 0.000075z - 0.101 \frac{n}{N}] + [0.498 + 0.00007z - 0.105 \frac{n}{N}] (\frac{n}{N})$ |
| El-Metwally | $R_s = 0.586R_0 + 1.74T_{\max} - 4.45T_{\min} - 355d_{cm} + 133$ |
| Hargreaves and Samani | $R_s R_0 = [0.00185(T_{\max} - T_{\min})^2 - 0.0433(T_{\max} - T_{\min}) + 0.4023] (T_{\max} - T_{\min})$ |
| Garg | $R_s R_0 = 0.348 + 0.448 \frac{n}{N} - 0.000083w_{at}$ |

R_s total radiation on a horizontal surface on the Earth's surface; n Actual number of solar radiation hours; N theoretical hours of solar radiation; RH relative humidity; T_{\max} and T_{\min} maximum and minimum air temperatures; cm average cloud cover (Okta); w_{at} content of atmospheric water vapor per unit volume of air

uncertainty in any of the required variables, the values are obtained from MOD / MYD08 products.

All of these files are saved in either GRID or Swath. After downloading the desired data, the obtained files with EOS-HDF extension are processed by HEG V2.12 software under Linux and the desired information layers are selected. These layers were then extracted into the Bash environment using the MODISStp package under the R programming language and converted to files with the TIFF extension. All MODIS data were geo-registered and resampled by the nearest neighborhood interpolation method, which was also performed using HEG V2.12. The required information was extracted from the layers using arcpy and os modules under the Python 2.7 programming language.

The total amount of daily radiation is estimated by determining the amount of momentary radiation at half-hour intervals using the Santa Barbara DISORT Atmospheric Radiative Transfer model. The momentary values in this model have an internal database including parameters such as diffuse reflection and absorption for clouds with liquid and solid droplets under different conditions. This database is based on the Mie Scattering Code and ranges from an effective radius of 2 to 128 micrometers. This code, which is actually the atmospheric transfer equation of radiation and is written in FORTRAN language, has physical models for calculating radiation under the influence of standard atmosphere, cloud, haze and surface (Liu et al. 2010). In this study, the effective radius values according to Liu et al. (2010) are considered as 10 μm for water droplets in the cloud and 65 μm for ice droplets belonging to the cloud, and the model with 4 flows by 0.005 Micrometer separation is implemented. Ozone and haze are 0.349 atm cm for the rural type. The short wavelength range is between 0.3 and 3 micrometers in proportion to the Pyranometer used in the stations. For cloudy skies, the total atmospheric water vapor is assumed to be 1.418 gr/cc, and the cloud cover is

homogeneously composed of parallel plates and is considered static during the morning and evening.

Based on these values and variables monitored at ground stations, the amount of momentary radiation at half-hour intervals is calculated. According to the surface altitude, atmospheric condition, solar tilt angle, and albedo of the earth surface for a given geographical position, the SBDART model is used to calculate direct and scattered radiation and the amounts of radiation in the form of downward shortwave flux for clear and cloudy skies are obtained. Atmospheric conditions include visibility, total water vapor, and visual thickness of the cloud. The model with a significant number of variables is designed so that there is a logical value instead of each variable which is not defined. The variables used in the present study includes Atmospheric Water Vapor (a.m. and p.m.), Cloud's Optical Depth (a.m. and p.m.), White sky albedo, Black sky albedo, Horizontal visibility and Aerosol for Kerman, Mashhad, Yazd and Zanjan in the 8-year period of 2015-2007.

These values are all obtained from MODIS products, except for the horizontal visibility variable, for which data were from the Meteorological Organization. These values indicate the atmospheric characteristics at two time points per day (10:30 and 13:30). The inclination angle of sun was also calculated for all intervals. The daily albedos were calculated by using interpolation operations between the two values of Black-sky Albedo and White-sky Albedo, as well, according to the change in the Zenith angle. The two partial values of albedo represent the albedo for the direct radiation and indirect radiation, respectively. In this way, each day is divided into three parts including sunrise up to 10:30 local time (Terra satellite transit time), 10:30 to 13:30 local time (Aqua transit time), and 13:30 until sunset. Then, the atmospheric characteristics of Terra and Aqua satellites were used for sections 1 and 3, while an interpolation was used for section 2. Since the maximum amount of radiation occurs in section 2, this interpolation increases the accuracy of the model.

The introduced empirical models were implemented on study stations for the selected days, as well. Observational

data were used for the values n/N , which are shown as Nn . Daily average cloud fraction (CF) data were used for estimating daily radiation by using Angstrom Prescott empirical model and the values of MOD/MYD08_D3 products were obtained. First, the images related to 50 days were downloaded for each station and their CF values were extracted. Since two values (morning and evening) were obtained for each day, the average for each day was taken. During the next step, by establishing a regression relation, an equation was obtained for calculating the value n/N using CF. The relations obtained for each station are presented in Table 3. Then, on the studied days, daily radiation values were obtained through the Angstrom-Prescott empirical model using CF values. The required coefficients of the Angstrom-Prescott empirical model for each station are considered according to Aghashariatmadari (2011).

Performance evaluation indices

There are various error indicators used to compare and assess the performance of models. In this research, in order to evaluate the performance of models against measured data, the most-routinely used indices including coefficient of determination (R^2), the mean absolute error (MAE), the root mean square error (RMSE), and the relative root mean square error (RRMSE) were used as follows:

- (1) Root-Mean-Square Error (RMSE):

$$RMSE = \left\{ \left[\sum_1^n (O_i - P_i)^2 \right] / n \right\}^{1/2} \tag{12}$$

- (2) Mean Bias Error (MBE)

$$MBE = \left[\sum_1^n (O_i - P_i) \right] / n \tag{13}$$

- (3) Coefficient of determination (R^2)

$$R^2 = 1 - \frac{RMSE^2}{\sigma^2} \tag{14}$$

Table 3 Regression relations between the average cloud fraction and sunny hours

| Station | Regression relationship | R^2 |
|---------|-------------------------|-------|
| Zanjan | CF=-1.103Nn+1.0433 | 0.83 |
| Kerman | CF=-1.166Nn+1.069 | 0.84 |
| Mashhad | CF=-1.116Nn+1.1127 | 0.61 |
| Yazd | CF=-1.13Nn+1.07 | 0.76 |

- (4) Mean Absolute Error (MAE)

$$MAE = \frac{1}{n} \sum_1^n |O_i - P_i| \tag{15}$$

- (5) Relative Root Mean Square Error (RRMSE)

$$RRMSE = \frac{\left\{ \left[\sum_1^n (O_i - P_i)^2 \right] / n \right\}^{1/2}}{1 / \sum_1^n P_i} \times 100 \tag{16}$$

- (6) Mean Absolute Percentage Error (MAPE):

$$MAPE = \frac{1}{n} \sum_{i=1}^n \left| \frac{P_i - O_i}{O_i} \right| \times 100 \tag{17}$$

where P_i indicates the estimated daily global solar radiation, O_i represents the observed values, σ is describes the standard deviation, and n considered as the number of the data pairs. The RMSE is a measure of random errors, which represents some information about the short-term performance of the regression. Knowing about the amount of RMSE and MAE is important because they represent errors in the units of the studied variables. The values of 1 in R^2 represent the better performance and perfect fit of the model, which is contrariwise in the case of RMSE and MAE indices (Badescu 2014). The MAPE indicates the mean absolute percentage difference between the estimated and measured data. Also, the RRMSE is obtained by dividing the root mean square error to the average of observed or measured data. Some studies such as Deo et al. (2018) and Ghorbani et al. (2018) indicated that different limits of this index is used to determine the accuracy of the models such as excellent for $RRMSE < 10\%$, good for $10\% < RRMSE < 20\%$, fair for $20\% < RRMSE < 30\%$, and poor for $RRMSE > 30\%$.

Results and discussion

In this study, the efficiency of a radiation estimation model was investigated by using satellite images compared to the Angstrom-Prescott empirical relation and eight selected empirical models of solar radiation estimation (Angstrom-Prescott model) and calibrated Angstrom-Prescott model, Swartman, Hargreaves & Samani, Gopinathan, Garg, and El-Metwally). After collecting data and preparing inputs, the models were implemented and the desired statistical indicators were calculated according to the amount of radiation measured with Pyranometers.

Evaluation the efficiency of models

Figure 2 shows the comparison between the calculated and estimated values of radiation using empirical models and parametric model (SBDART) and the values of statistical error indices of the studied models in general and by station are presented in Table 4 and Fig. 2.

As illustrated in Fig. 2 and Table 4, the coefficients of determination vary between 0.25 and 0.95, most of which

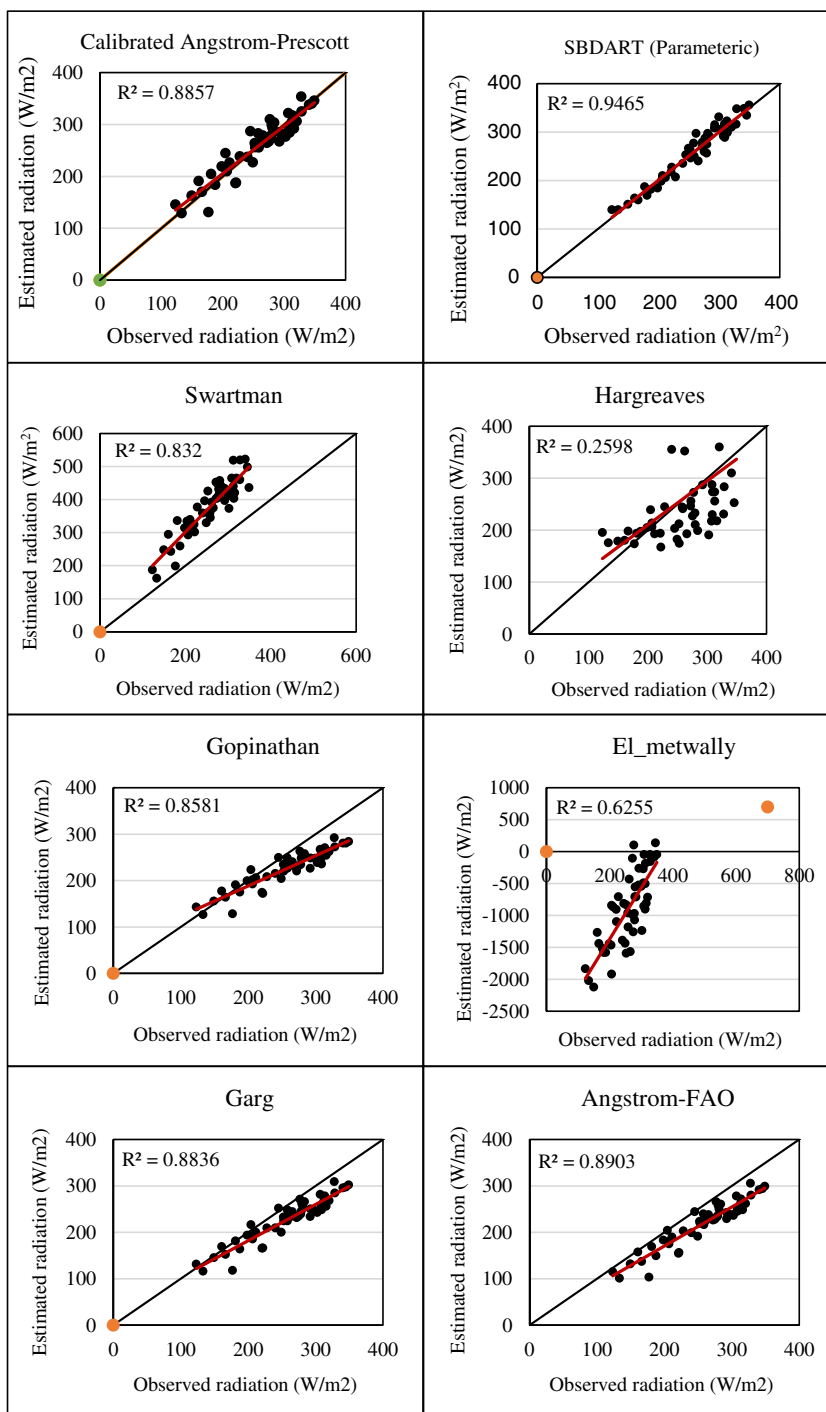
are related to the SBDART (Parametric) model and the least of which are related to the Hargreaves model. After SBDART model, the highest R^2 values are related to calibrated Angstrom and Angstrom-FAO models ($R^2 = 0.89$), Garg model ($R^2 = 0.88$) and Gopinathan model ($R^2 = 0.86$), respectively. In addition, the mean absolute error percentage of the SBDART model is significantly different from other models (MAPE = 4.3%). After the parametric model, the lowest MAPE is related to the Angstrom model (MAPE = 5.98%).

Table 4 Calculated statistical indices of models

| | | Calibrated Angstrom | SBDART | Swartman | Hargreaves | Gopinathan | El-Metwally | Garg | FAO Angstrom |
|---------|--------------------------|---------------------|--------|----------|------------|------------|-------------|-------|--------------|
| Zanjan | RMSE (W/m ²) | 18.1 | 10.4 | 79.5 | 77.4 | 34.7 | 1162.7 | 34.7 | 73.1 |
| | MBE(W/m ²) | 3.6 | -1.3 | -61.9 | -13.0 | 23.2 | 920.0 | 23.2 | 55.8 |
| | t | 0.7 | 0.46 | 4.5 | 0.6 | 3.2 | 4.7 | 3.3 | 30.7 |
| | R ² | 0.90 | 0.97 | 0.83 | 0.42 | 0.87 | 0.73 | 0.87 | 0.85 |
| | MAPE% | 7.4 | 3.9 | 36.3 | 17.3 | 12.7 | 624.2 | 12.7 | 19.8 |
| | MAE(W/m ²) | 16.6 | 10.97 | 78.7 | 44.2 | 29.7 | 1170.9 | 29.7 | 55.8 |
| | RRMSE% | 7.1 | 6 | 46.3 | 45.1 | 20.2 | 676.7 | 20.2 | 42.6 |
| Yazd | RMSE (W/m ²) | 7.92 | 10.38 | 128.5 | 41.92 | 36.31 | 1116.9 | 30.59 | 35.35 |
| | MBE(W/m ²) | 0.11 | 2.36 | -102.5 | 27.56 | 25.47 | 814.01 | 22.86 | 27.62 |
| | t | 0.05 | 0.87 | 4.94 | 3.26 | 3.68 | 3.98 | 4.2 | 4.68 |
| | R ² | 0.86 | 0.97 | 0.89 | 0.64 | 0.92 | 0.73 | 0.86 | 0.86 |
| | MAPE% | 14.79 | 3.9 | 44.2 | 23.9 | 13.4 | 495.1 | 11.6 | 15.09 |
| | MAE(W/m ²) | 7.54 | 10.89 | 139.77 | 39.82 | 36.37 | 1110.02 | 31.17 | 7.96 |
| | RRMSE% | 1.98 | 4.08 | 50.5 | 16.5 | 14.3 | 439.3 | 12.03 | 13.9 |
| Mashhad | RMSE (W/m ²) | 23.1 | 13.13 | 113.0 | 63.5 | 40.6 | 1272.6 | 37.9 | 44.2 |
| | MBE(W/m ²) | -0.2 | 2.55 | -107.8 | 33.1 | 29.5 | 1155.0 | 29.5 | 38.3 |
| | t | 0.0 | 0.59 | 9.5 | 1.8 | 3.2 | 15.4 | 3.7 | 5.2 |
| | R ² | 0.86 | 0.96 | 0.89 | 0.23 | 0.84 | 0.62 | 0.86 | 0.86 |
| | MAPE% | 14.8 | 5.03 | 44.2 | 23.9 | 14.8 | 446.4 | 13.2 | 15.1 |
| | MAE(W/m ²) | 20.0 | 11.37 | 98.0 | 51.2 | 33.9 | 1155.0 | 30.3 | 7.4 |
| | RRMSE% | 9.3 | 5.8 | 5.0 | 28.1 | 18.0 | 20.0 | 16.8 | 19.6 |
| Kerman | RMSE (W/m ²) | 21.1 | 14.46 | 126.8 | 99.5 | 45.5 | 1086.4 | 42.7 | 22.7 |
| | MBE(W/m ²) | 5.8 | -2.53 | -124.8 | -57.7 | 37.3 | 981.8 | 36.5 | 9.5 |
| | t | 0.9 | 0.56 | 15.7 | 2.3 | 4.4 | 6.7 | 5.2 | 3.3 |
| | R ² | 0.89 | 0.89 | 0.89 | 0.42 | 0.83 | 0.53 | 0.86 | 0.86 |
| | MAPE% | 7.2 | 4.061 | 46.7 | 27.4 | 14.5 | 428.9 | 14.0 | 16.7 |
| | MAE(W/m ²) | 17.8 | 11.16 | 124.4 | 73.6 | 40.1 | 981.8 | 38.0 | 9.5 |
| | RRMSE% | 8.1 | 5.5 | 48.6 | 38.1 | 17.4 | 4.2 | 16.3 | 8.7 |
| Total | RMSE (W/m ²) | 19.3 | 13.5 | 126.8 | 81.5 | 40.6 | 1272.6 | 36.9 | 43.3 |
| | MBE(W/m ²) | -0.5 | -0.6 | -120.8 | -1.0 | 32.1 | 1155.0 | 30.8 | 38.9 |
| | t | 0.2 | 0.3 | 22.5 | 0.1 | 9.2 | 15.4 | 10.8 | 14.6 |
| | R ² | 0.89 | 0.95 | 0.83 | 0.25 | 0.86 | 0.62 | 0.88 | 0.89 |
| | MAPE% | 6.0 | 4.3 | 46.7 | 23.2 | 13.5 | 446.4 | 12.4 | 15.0 |
| | MAE(W/m ²) | 15.5 | 11.1 | 120.8 | 60.2 | 35.0 | 1155.0 | 32.1 | 38.9 |
| | RRMSE% | 7.5 | 5.2 | 48.9 | 31.5 | 15.7 | 491.2 | 14.2 | 16.7 |

RMSE root-mean-square error; MBE mean bias error; R²: coefficient of determination; MAPE mean absolute percentage error; MAE mean absolute error, and RRMSE relative root mean square

Fig. 2 Output distribution of models versus the values observed at the studied stations



The MAPE measurement value for other models is higher than 12% and the highest percentage of mean absolute error is related to the El-Metwally model with the rate 446.4. Furthermore, the relative root mean square error (RRMSE) is equal to 5.2% and 7.5% for the SBDART and calibrated Angstrom models, respectively. For other statistical error indicators, the SBDART model performs significantly better than other models.

Figure 2 shows how the calculated data are distributed around the bisector line. As shown, only the SBDART model and then the calibrated Angstrom model have little scattering of points around the bisector line. The highest scatter rate is related to Hargreaves and El-Metwally models, whose error indices were higher in Table 4 than other models. The RMSE values of different models vary based on the overlapped data of all stations studied in the range 13.5–1272.6 W/m²day.

At Zanjan station, the RMSE values of different models change in the range of 10.4–1162.7 W/m².day. The lowest mean absolute percentage error (MAPE) is equal to 3.9% and the highest rate of coefficient of determination (*R*²) is equal to 0.97 and both indicators are related to the SBDART model. The calibrated Angstrom model with values of MAPE = 7.4% and *R*² = 0.9 after the parametric model has a better estimate of solar radiation at this station. At Yazd station, SBDART model with a considerable difference from other models with MAPE=3.9% and *R*²=0.97 have the best estimate of solar radiation in this station. Statistical indices of SBDART model of Mashhad station indicated a better estimate of this model than other models (MAPE = 4.3% and *R*² = 0.96). In a similar situation for Kerman station, SBDART model with indices of MAPE = 4.7% and *R*² = 0.95 has better performance than experimental models. In terms of RMSE index, the best performance is related to the parametric model, and the Angstrom-PreScott empirical model using satellite data has the highest error compared to the studied models like the coefficient of determination index. This is also not the case with Kerman station, and seems to be related to the fact that satellite data related to the daily average cloud fraction (CF) fit well with sunshine hour data (Table 3).

Combining empirical models and satellite data

The results of statistical analysis of empirical models show that the increase in model variables does not necessarily increase their accuracy and the estimation of models with less input such as Angstrom model is more accurate than other models. On the other hand, as shown in Table 5, by comparing the three models of Angstrom Prescott based on station observations, the parametric model and Angstrom based on satellite data on different days in terms of fraction of sunshine hours (cloudy and cloudless day), the parametric model is more efficient on cloudy days than on cloudless days so that the calculated RMSE and MBE indices for cloudy days are 9.07 W/m².day and - 0.72 W/m².day, and are 19.77 W/m².day and 3.60 W/m².day, respectively, for sunny days. In contrast, the empirical Angstrom-PreScott model had better results with observational data on cloudless days so that the indices were RMSE = 43.60 W/m².day and MBE = 34.25 W/m².day for cloudy days, and were RMSE = 29.56 W/m².day and = MBE

= 6.19 W/m².day for cloudless days. With the calculated indices for the Angstrom-PreScott model with satellite data, it is not possible to judge whether it is different or insensitive to cloudy or sunny days. Furthermore, this model has not been very sensitive to nNchanges.

Sensitivity analysis of models

The sensitivity of empirical solar radiation models to meteorological variables was analyzed. The implemented method is based on changing the meteorological value by a defined percentage steps and computing the corresponding percentage change in *R*_s while keeping the other variables constant at their long-term averages. This was accomplished in the study area by changing the variables from -20 to + 20% with ± 5% increments that were deemed to influence *R*_s. These variables included: *T*_{max}, *T*_{min}, RH_{mean}%, cloudiness, Hourly Vapor Pressure (hvp) and sunshine hours.

Figure 3 shows the relative change in *R*_s due to the relative change in a selected meteorological variable. As it can be seen in the figure, in Calibrated Angstrom-FAO model, in response to the change in n/N by 20%, *R*_s changed about 10%. This value was about 11% for n/N in main Angstrom-FAO model. As well as, for Gopinatan model, a 20% change in n/N led to a 7.1% change in *R*_s. In the case of El-Metwally model, this value was about 28% for the cloudiness and about 1.1% and 1.4% for *T*_{max} and *T*_{min}, respectively. Also, For Swartman model, with n/N and RH_{mean} variables, *R*_s had the highest sensitivity to n/N with a change of 7%. Furthermore, it can be seen at the Garg model, in response to the change in hvp by 20%, *R*_s varied about 30%. This value is about 20% for n/N. And finally in Hargreaves model the highest changes of *R*_s is belong to *T*_{max} by value of 34 % in comparison with 12.5% variation in response to a 20% change in *T*_{min}.

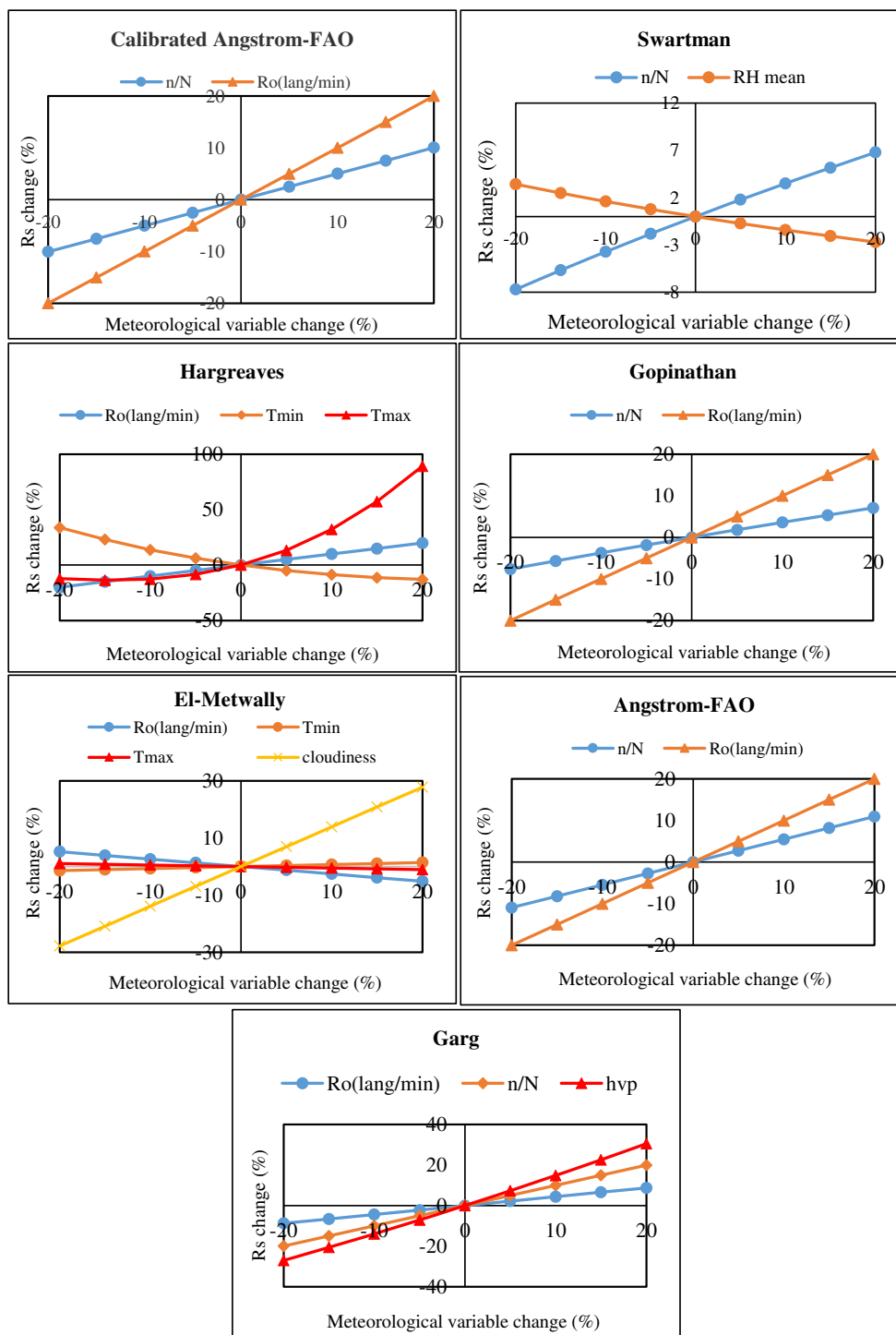
Conclusion

The present study proposed a satellite based method based on SBDART algorithm to predict the global solar radiation in target stations with more accuracy. The ability to collect continuous temporal and spatial signals above the atmosphere is considered as one of the advantages of remote sensing and

Table 5 Comparison of models in different sky conditions in terms of cloud cover

| Model | Angstrom-PreScott (Satellite based) | | Angstrom-PreScott (observational based) | | Parametric | |
|-------|-------------------------------------|--------------------------|---|--------------------------|--|--------------------------|
| | MBE (W/m ²) | RMSE (W/m ²) | MBE (W/m ²) | RMSE (W/m ²) | MBE(W/m ²) (W/m ²) | RMSE (W/m ²) |
| Nn | | | | | | |
| 0.5< | 19.70 | 41.74 | 34.25 | 43.60 | -0.72 | 9.07 |
| 0.5> | 18.39 | 44.97 | 6.19 | 29.56 | 3.60 | 19.77 |

Fig. 3 Percent change in R_s vs. percent changes in meteorological variables



satellite images. Also, the minimum data requirement is considered as another key advantage of this method, especially in data-scarce regions. This feature makes it possible to estimate radiation in remote areas where radiation stations are scattered. In addition to being more accurate nationwide (rather than point-to-point), satellite data have far lower costs. Each of the two satellite based methods used here have advantages and disadvantages. The parametric model is accurate for

different sky conditions ($R^2 = 95\%$ and $RRMSE = 5.2\%$) and only uses satellite data without any need of other meteorological data. However, its complexity, having a large number of input variables, as well as being time consuming (especially due to the lack of access to high-speed computer systems) are considered as its weaknesses. On the other hand, the satellite based Angstrom-PreScott model has no complexity in the process and requires a small number of variables thus it can be

easily used for different areas. This model needs accurate sunshine hour's data and requires calibration of relationship coefficients for the study area. However, its lower accuracy relative to the parametric model ($R^2 = 0.57$ and $RRMSE = 16.9\%$) in some precise applications may not yield good results. Based on the findings of this study, the proposed satellite based method is highly efficient in predicting global solar radiation values. By considering the importance of solar radiation values, the performance of other modern models can be evaluated for simulating this variable. Due to the difference in model efficiency in different climatic conditions, it is suggested that the applicability of introduced parametric model is also evaluated in different climate conditions.

Declarations

Conflict of interest The authors declare that they have no competing interests.

References

- Aghashariatmadari Z (2011) Evaluation of model for estimating total solar radiation at horizontal surfaces based on meteorological data, with emphasis on the performance of the angstrom model over Iran. Ph. D. Dissertation, University of Tehran
- Allen RG, Pereira LS, Raes D, Smith M (1998) Crop evapotranspiration: Guidelines for computing crop water requirements. Food and Agriculture Organization, Rome, Italy: FAO Irrigation and Drainage
- Alsina EF, Bortolini M, Gamberi M, Regattieri A (2016) Artificial neural network optimization for monthly average daily global solar radiation prediction. *Energy Convers Manag* 120:320–329. <https://doi.org/10.1016/j.enconman.2016.04.101>
- Angstrom A (1924) Solar and terrestrial radiation. *QIR Meteorol Soc* 50(210):121–126. <https://doi.org/10.1002/qj.49705021008>
- Badescu V (2014) Modeling solar radiation at the earth's surface. Springer, Verlag Berlin Heidelberg
- Bamehr S, Sabetghadam S (2021) Estimation of global solar radiation data based on satellite-derived atmospheric parameters over the urban area of Mashhad, Iran. *Environ Sci Pollut Res* 28(6):7167–7179. <https://doi.org/10.1007/s11356-020-11003-8>
- Benajes J, Martín J, García A, Villalta D, Warey A (2015) In-cylinder soot radiation heat transfer in direct-injection diesel engines. *Energy Convers Manag* 106:414–427. <https://doi.org/10.1016/j.enconman.2015.09.059>
- Cano DJ, Monget M et al (1986) A method for the determination of the global solar radiation from meteorological satellite data. *Sol Energy* 37(1):31–39. <https://doi.org/10.1016/j.rser.2017.01.114>
- Chen JL, Li GS, Xiao BB, Wen ZF, Lv MQ, Chen CD, Jiang Y, Wang XX, Wu SJ (2015) Assessing the transferability of support vector machine model for estimation of global solar radiation from air temperature. *Energy Convers Manag* 89:318–329. <https://doi.org/10.1016/j.enconman.2014.10.004>
- Chen X, Xia XL, Liu H, Li Y, Liu B (2016) Heat transfer analysis of a volumetric solar receiver by coupling the solar radiation transport and internal heat transfer. *Energy Convers Manag* 114:20–27. <https://doi.org/10.1016/j.enconman.2016.01.074>
- Demirhan H, Menteş T, Atilla M (2013) Statistical comparison of global solar radiation estimation models over Turkey. *Energy Convers Manag* 68:141–148. <https://doi.org/10.1016/j.enconman.2013.01.004>
- Deo R, Sahin M (2017) Forecasting long-term global solar radiation with an ANN algorithm coupled with satellite-derived (MODIS) land surface temperature (LST) for regional locations in Queensland. *Renew Sust Energ Rev* 72:828–848. <https://doi.org/10.1016/j.rser.2017.01.114>
- Deo RC, Ghorbani MA, Samadianfard S, Maraseni T, Bilgili M, Biazar M (2018) Multi-layer perceptron hybrid model integrated with the firefly optimizer algorithm for windspeed prediction of target site using a limited set of neighboring reference station data. *Renew Energy* 116:309–323. <https://doi.org/10.1016/j.renene.2017.09.078>
- El-Metwally M (2004) Simple new methods to estimate global solar radiation based on meteorological data in Egypt. *Atmos Res* 69: 217–239. <https://doi.org/10.1016/j.atmosres.2003.09.002>
- Gao B et al (2015) MODIS Atmosphere L2 Water Vapor Product. NASA MODIS Adaptive Processing System. Goddard Space Flight Center, Greenbelt. https://doi.org/10.5067/MODIS/MOD05_L2.006
- Garg H, Garg S (1982) Prediction of solar radiation from bright sunshine and other parameters. *Energy Convers Manag* 23(2):113–118. [https://doi.org/10.1016/0196-8904\(83\)90070-5](https://doi.org/10.1016/0196-8904(83)90070-5)
- Gautier C, Diak G, Masse S (1980) A simple physical model to estimate incident solar radiation at the surface from Goes satellite data. *J Appl Meteorol* 19:1005–1012. [https://doi.org/10.1175/1520-0450\(1980\)019%3C1005:ASPMTE%3E2.0.CO;2](https://doi.org/10.1175/1520-0450(1980)019%3C1005:ASPMTE%3E2.0.CO;2)
- Ghimire S, Deo RC, Raj N, Mi J (2019) Deep learning neural networks trained with MODIS satellite-derived predictors for long-term global solar radiation prediction. *Energies* 12(12):2407
- Ghorbani MA, Deo RC, Yaseen ZM, Kashani MH, Mohammadi B (2018) Pan evaporation prediction using a hybrid multilayer perceptron-firefly algorithm (MLP-FFA) model: case study in North Iran. *Theor Appl Climatol* 133:1119–1131. <https://doi.org/10.1007/s00704-017-2244-0>
- Gopinathan KK (1988) A simple method for predicting global solar radiation on a horizontal surface. *Sol Wind Technol* 5:581–586. [https://doi.org/10.1016/0741-983X\(88\)90050-1](https://doi.org/10.1016/0741-983X(88)90050-1)
- Hargreaves G, Samani Z (1982) Estimating potential evapotranspiration. *J Irrig Drain Eng ASCE* 108:225–230
- Hussain M (1984) Estimation of global and diffuse irradiation from sunshine duration and atmospheric water vapor content. *Sol Energy* 33: 217–220. [https://doi.org/10.1016/0038-092X\(84\)90240-8](https://doi.org/10.1016/0038-092X(84)90240-8)
- Janjai S, Laksanaboonsong J, Nunez M, Thongsathitya A (2005) Development of a method for generating operational solar radiation maps from satellite data for a tropical environment. *Sol Energy* 78: 739–751. <https://doi.org/10.1016/j.solener.2004.09.009>
- Joumeé M, Bertrand C (2010) Improving the spatio-temporal distribution of surface solar radiation data by merging ground and satellite measurements. *Remote Sens Environ* 114:2692–2704. <https://doi.org/10.1016/j.rse.2010.06.010>
- Kim HY, Liang S (2010) Development of a hybrid method for estimating land surface shortwave net radiation from MODIS data. *Remote Sens Environ* 114(11):2393–2402. <https://doi.org/10.1016/j.rse.2010.05.012>
- Liu X, Mei X, Li Y, Porter JR, Wang Q, Zhang Y (2010) Choice of the Ångström–Prescott coefficients: Are time-dependent ones better than fixed ones in modeling global solar irradiance? *Energy Convers Manag* 51(12):2565–2574. <https://doi.org/10.1016/j.enconman.2010.05.020>
- López G, Batlles F (2014) Estimating Solar Radiation from MODIS Data. *Energy Procedia* 49:2362–2369. <https://doi.org/10.1016/j.egypro.2014.03.250>
- Lotfi H (2012) Evaluation of net radiation with use of MODIS sensor data. Dissertation, Agricultural Faculty of Shiraz University.
- Mohammadi B, Aghashariatmadari Z (2020) Estimation of solar radiation using neighboring stations through hybrid support vector regression

- boosted by Krill Herd algorithm. Arab J Geosci 13:1–16. <https://doi.org/10.1007/s12517-020-05355-1>
- Moradi I, Mueller R, Alijani B, Ga K (2009) Evaluation of the Heliosat-II method using daily irradiation data for four stations in Iran. Sol Energy 83(2):150–156. <https://doi.org/10.1016/j.solener.2008.07.010>
- Muneer T (2004) solar radiation and daylight models. Elsevier, Burlington
- Perez R, Seals R, Zelenka A (1997) Comparing satellite remote sensing and ground network measurements for the production of site/time specific irradiance data. Sol Energy 60:89–96. [https://doi.org/10.1016/S0038-092X\(96\)00162-4](https://doi.org/10.1016/S0038-092X(96)00162-4)
- Perez R, Ineichen P, Moore K, Kmiecik M, Chain C, George R, Vignola F (2002) A new operational model for satellite-derived irradiances: description and validation. Sol Energy 73(5):307–317. [https://doi.org/10.1016/S0038-092X\(02\)00122-6](https://doi.org/10.1016/S0038-092X(02)00122-6)
- Prescott J (1940) Evaporation from a water surface in relation to solar radiation. Trans Roy Soc S Aust 46:114–125
- Qin J, Chen Z, Yang K, Liang S, Tang W (2011) Estimation of monthly-mean daily global solar radiation based on MODIS and TRMM products. Appl Energy 88(7):2480–2489. <https://doi.org/10.1016/j.apenergy.2011.01.018>
- Raschke R, Preuss H (1979) The determination of the solar radiation budget at the earth surface from satellite measurements. Meteorol Rundsch 32:18
- Renno C, Petito F, Gatto A (2015) Artificial neural network models for predicting the solar radiation as input of a concentrating photovoltaic system. Energy Convers Manag 106:999–1012. <https://doi.org/10.1016/j.enconman.2015.10.033>
- Ricchiuzzi P, Yang S, Gautier C, Sowle D (1998) SBDART: A research and teaching software tool for plane-parallel radiative transfer in the Earth's atmosphere. Bulletin of the American Meteorological Society 79(10):2101–2114
- Rigollier C, Lefèvre M, Wald L (2004) The method Heliosat-2 for deriving shortwave solar radiation from satellite images. Sol Energy 77: 159–169. <https://doi.org/10.1016/j.solener.2004.04.017>
- Ryu Y, Jiang C, Kobayashi H, Detto M (2018) MODIS-derived global land products of shortwave radiation and diffuse and total photosynthetically active radiation at 5 km resolution from 2000. Remote Sens Environ 204:812–825. <https://doi.org/10.1016/j.rse.2017.09.021>
- Schillings C, Mannstein H, Meyer R (2004a) Operational method for deriving high resolution direct normal irradiance from satellite data. Sol Energy 76:475–484. <https://doi.org/10.1016/j.solener.2003.07.038>
- Schillings C, Meyer R, Mannstein H (2004b) Validation of a method for deriving high resolution direct normal irradiance from satellite data and application for the Arabian Peninsula. Sol Energy 76:487–497. <https://doi.org/10.1016/j.solener.2003.07.037>
- Sun H, Zhao N, Zeng X, Yan D (2015) Study of solar radiation prediction and modeling of relationships between solar radiation and meteorological variables. Energy Convers Manag 105:880–890. <https://doi.org/10.1016/j.enconman.2015.08.045>
- Swartman RK, Ogunlade O (1967) Solar radiation estimates from common parameters. Sol Energy 11:170–172. [https://doi.org/10.1016/0038-092X\(67\)90026-6](https://doi.org/10.1016/0038-092X(67)90026-6)
- Tamm E, Thomalla E (1992) Handbook of Helionda: a program to simulate the effects of Meteorology, Place and Time. Jülich: BMFT-Forschungsprojekt 0328932A
- Tarpley J (1979) Estimating Incident Solar-Radiation at the Surface from Geostationary Satellite Data. J Appl Meteorol 18(9):1172–1181. [https://doi.org/10.1175/1520-0450\(1979\)018%3C1172:EISRAT%3E2.0.CO;2](https://doi.org/10.1175/1520-0450(1979)018%3C1172:EISRAT%3E2.0.CO;2)
- Yang K, Koike T, Ye B (2006) Improving estimation of hourly, daily, and monthly solar radiation by importing global data sets. Agric For Meteorol 137(1-2):43–55. <https://doi.org/10.1016/j.agrformet.2006.02.001>
- Zelenka A, Perez R, Seals R, Renné D (1999) Effective Accuracy of Satellite-Derived Hourly Irradiances. Theor Appl Climatol 62(3-4):199–207. <https://doi.org/10.1007/s007040050084>
- Zhang X, Liang S, Zhou G, Wu H, Zhao X (2014) Generating Global and Surface Satellite incident shortwave radiation and photosynthetically active radiation products from multiple satellite data. Remote Sens Environ 152:318–332. <https://doi.org/10.1016/j.rse.2014.07.003>